NASA Technical Memorandum 100119

An Analytical and Experimental Study of Injection-Locked Two-Port Oscillators

Jon C. Freeman and Alan N. Downey
Lewis Research Center
Cleveland, Ohio

July 1987

NASA

AN ANALYTICAL AND EXPERIMENTAL STUDY OF INJECTION-LOCKED

TWO-PORT OSCILLATORS

Jon C. Freeman and Alan N. Downey
National Aeronautics and Space Administration
Lewis Research Center
Cleveland, Ohio 44135

SUMMARY

A Ku-band IMPATT oscillator with two distinct output power ports was injection-locked alternately at both ports. The transmission locking bandwidth was nearly the same for either port. The lower free running power port had a reflection locking bandwidth that was narrower than its transmission locking one. Just the opposite was found at the other port. A detailed analytical model for two-port injection-locked oscillators is presented, and its results agree quite well with the experiments. A detailed critique of the existing literature on this topic is included to clear up several misconceptions and errors that have appeared in several articles. It is concluded that two-port injection-locked oscillators may prove useful in certain communication systems.

INTRODUCTION

This report is concerned with the injection locking properties of two-port oscillators. This type of oscillator differs from the more common one-port, in that power is simultaneously delivered to two separate loads. This configuration has several advantages over the conventional one-port, and these can be especially useful in millimeter wave bands. These advantages can be visualized by considering the following two examples. The first example involves a W-band millimeter-wave receiver with GaAs or InP GUNN diode local oscillators (refs. 1 and 2). These oscillators have two ports and are operated at a fundamental frequency of 80 GHz. Furthermore, these oscillators are injection locked by a subharmonic of the fundamental frequency, that is, 40 GHz. The subharmonic signal is coupled to the GUNN diode through a circulator at the second port of the oscillator. Thus with a two-port oscillator the circulator, which requires considerable innovation to design and fabricate, operates at a much lower frequency corresponding to the subharmonic. This is clearly an advantage over a single-port oscillator which requires the circulator to operate at the fundamental frequency. The second example involves reduction of noise and drift in two-port GUNN oscillators by self-locking through a phase locked loop (PLL). In this case a small fraction of the oscillator power is coupled via the second port to the PLL to stabilize the bias. Once again when compared with a single-port oscillator, with an external directional coupler, the above scheme offers considerable simplification of the receiver design. Figure 1 schematically illustrates the above two examples.

In references 3 to 7 injection locking properties of GaAs metal semiconductor field effect transistor (MESFET) two-port oscillators has been presented. Some of their results and interpretations are erroneous and misleading. For example they infer that a circulator is not always necessary at the injection port. We show in detail that such a condition is highly questionable and not borne out by their experiments. Secondly, the enhancement of

locking bandwidth from one port to the other is due strictly to the ratio of $|S_{21}/S_{12}|$ and thus unilateral oscillators (nontransistor) i.e., GUNN and IMPATT devices, do not show the increased locking bandwidth they find with the MESFET based oscillators. In reference 7 some experiments are misinterpreted and mistakenly show such enhancement for GUNN oscillators.

In this paper/report we wish to clear the above confusion by demonstrating analytically as well as experimentally the relationship between the locking bandwidth and the locking gain of a two-port injection-locked oscillator. A lumped element equivalent circuit model is used to represent the circulator, the two-ports of the oscillator, and the IMPATT diode for the purpose of circuit analysis. The experiments are conducted on a Ku-band two-port IMPATT diode oscillator. The silicon IMPATT diodes used in the experiments have a flat profile and are of the single drift type. Our studies show that the locking bandwidth is the same, for identical locking gain, when locked from either channel. Further, the transmission locking bandwidth is larger than the reflection locking bandwidth when the lower free-running output channel is the side at which the injected signal is applied. Just the opposite case occurs when injected from the other port.

VARIOUS INJECTION LOCKING TECHNIQUES

Figure 2 serves to define the concepts of reflection locking (RL) and transmission locking (TL). A reflection locked oscillator (RLO), part (a), is basically the normal locking arrangement used for one-ports. The oscillator power delivered to the normal load is P_{02}. The power delivered to the "other" load is P_{01}. In a normal one-port, the "other" load is not present. The matching network, M, in the drain lead and the circulator are integral parts of the oscillator. Part (b) depicts the transmission locked oscillator (TLO). This technique injects the locking signal at the "other" (usually lower power) port. Tajima and Mishima (refs. 3 to 6) have studied these configurations using GaAs FET devices. Their basic conclusion is that one may achieve a wider locking range for the same level of injection power P_{inj} by using the TLO configuration rather than the one for RLO.

Many other useful properties of the TLO are expanded upon in appendix B, where their work is thoroughly reviewed. A careful review of their work is necessary, as several misleading and confusing statements and conclusions were made. Some of this confusion lead to further experimentation by Rajput and Sarkar (ref. 7); wherein misleading conclusions concerning two-port injection locking were reported. Their work is critiqued in appendix C.

ANALYTICAL EXPRESSIONS FOR LOCKING BANDWIDTHS

Background material on injection locked oscillators may be found in the articles by Kurokawa (refs. 9 to 11), and Hayasaka et al. (ref. 13). Here we consider the locking of single drift IMPATT two-port oscillators. When a negative resistance device is locked, both the impedance and output power change slightly from their free-running values. As a result, the standing wave patterns in the microwave circuit change somewhat. The shift in impedance at all points in the network causes a change in the power delivered to the loads. The model used to study this behavior is given in figure 3. For simplicity the turns ratios are assumed constant throughout the locking bandwidth. Initially

we neglect the variation of device reactance with rf voltage, and assume the device conductance may be approximated by (ref. 14)

$$g(V) = G_M \left(1 - \frac{V}{V_M}\right) \tag{1}$$

which is very reasonable for IMPATTS. Nearly all studies of oscillator locking behavior essentially linearize the device negative resistance or conductance, so equation (1) is not a prohibitive relationship. The effects of device reactance change will be incorporated later in a straightforward manner.

From the results of appendix A, the two-port configuration may be modeled as shown in part (b) of figure 3. By inspection we obtain

$$i_D = 2mi_L - m^2 Y_0 V \tag{2}$$

$$i_R = ni_b = n^2 Y_0 V \tag{3}$$

$$i' = i_D - i_R = -gV + C\frac{dV}{dt} + \frac{1}{L}\int V dt \tag{4}$$

or

$$\left(m^2 Y_0 + n^2 Y_0 - g\right)V + C\frac{dV}{dt} + \frac{1}{L}\int V dt = 2mi_L \tag{5}$$

which is the basic differential equation for a two-port oscillator. It is the same as equation (A23) with the addition of the term $n^2 Y_0$. Using the slowly varying assumptions (see appendix A) we obtain

$$\left(m^2 Y_0 + n^2 Y_0 - g\right)V_0 + C\frac{dV_0}{dt} + \frac{1}{\omega^2 L}\frac{dV_0}{dt} = 2mI_0 \cos\varphi \tag{6}$$

$$-cV_0\left(\omega + \frac{d\varphi}{dt}\right) + \frac{1}{\omega^2 L}\left(\omega V_0 - V_0\frac{d\varphi}{dt}\right) = 2mI_0 \sin\varphi \tag{7}$$

where $V(t)$ and $i_L(t)$ are defined in the appendix. In steady-state, equation (7) yields

$$(\omega_0 - \omega) \doteq \frac{mI_0 L \sin\varphi}{V_0} \omega_0^2 \tag{8}$$

which is the fundamental expression for the locking bandwidth. If one were to injection lock from port 2, the only change would be the replacement of m by n, the turns ratio at port 2.

We shall define several locking bandwidths depending upon the port the injection source is placed, and which load power level we choose to use. With

3

reference to Tajima and Mishima's work (see appendix B) we will define reflection locking as the case wherein the injector is at port 2. We use P_{02}, the power into the load at port 2, to express V_0,

$$V_0 = \frac{1}{n}\sqrt{\frac{P_{02}}{Y_0}} \tag{9}$$

For I_0 we have

$$I_0 = \sqrt{Y_0 P_{inj}} \tag{10}$$

Using equations (9) and (10) into equation (8) with m replaced by n since the injector is at port 2, we have

$$(\omega_0 - \omega)_{RL} = \omega_0^2 Ln^2 Y_0 \sqrt{\frac{P_{inj}}{P_{02}}} \sin \varphi$$

or the total half-locking range $\left. LR \right|_{RL} \stackrel{\Delta}{=} BW_{RL}^{(2)}$ as

$$BW_{RL}^{(2)} = \omega_0^2 Ln^2 Y_0 \sqrt{\frac{P_{inj}}{P_{02}}} \tag{11}$$

where the 2 in parentheses indicates the port at which the injection source is applied. Also their definition of transmission locking would mean placing the injector at port 1 and still using P_{02} to express V_0. Thus equations (8), (9), and (10) give

$$BW_{TL}^{(1)} = \omega_0^2 LnmY_0 \sqrt{\frac{P_{inj}}{P_{02}}} \tag{12}$$

where in both cases, the same value for P_{inj} has been used. This restraint is necessary in their work (see appendix B). Thus

$$\frac{BW_{TL}^{(1)}}{BW_{RL}^{(2)}} = \frac{m}{n} = \sqrt{\frac{P_{01}}{P_{02}}} \tag{13}$$

since

$$P_{01} = m^2 V_0^2 Y_0 \tag{14}$$

$$P_{02} = n^2 V_0^2 Y_0 \tag{15}$$

Notice that equation (13) is exactly their result, equation (B-24), for a bilateral device, which applies here for the IMPATT.

For purposes of relating the above to experimental results we shall define the following locking bandwidths. For the injection source at port 1:

$$BW_{RL}^{(1)} = \omega_o^2 Lm^2 Y_o \sqrt{\frac{P_{inj_1}}{P_{01}}} \qquad (16)$$

$$BW_{TL}^{(1)} = \omega_o^2 Lmn \, Y_o \sqrt{\frac{P_{inj_1}}{P_{02}}} \qquad (17)$$

when at port 2:

$$BW_{RL}^{(2)} = \omega_o^2 Ln^2 Y_o \sqrt{\frac{P_{inj_2}}{P_{02}}} \qquad (18)$$

$$BW_{TL}^{(2)} = \omega_o^2 Lmn \, Y_o \sqrt{\frac{P_{inj_2}}{P_{01}}} \qquad (19)$$

Therefore

$$\frac{BW_{TL}^{(1)}}{BW_{TL}^{(2)}} = \frac{\sqrt{\dfrac{P_{inj_1}}{P_{02}}}}{\sqrt{\dfrac{P_{inj_2}}{P_{01}}}} \qquad (20)$$

and if the locking gains are equal, where the locking gains are defined as,

$$LG_{21} = \sqrt{\frac{P_{01}}{P_{inj_2}}} \, , \text{ etc}$$

we have

$$BW_{TL}^{(1)} = BW_{TL}^{(2)} \qquad (21)$$

The experimental results of Rajput and Sarkar (ref. 7) can now be discussed in detail. Essentially they performed reflection locking at port 2, then transmission locking at port 1. The ratio of these locking ranges (bandwidths) is that obtained from equations (18) and (17)

$$\frac{BW_{RL}^{(2)}}{BW_{TL}^{(1)}} = \sqrt{\frac{P_{inj_2}}{P_{inj_1}}} \sqrt{\frac{P_{02}}{P_{01}}} = \frac{LG_{12}}{LG_{21}} \qquad (22)$$

5

But they actually changed their circuit between the two experiments. During RL they set $P_{01} = 0$ whereas during TL they used both P_{01} and P_{02}. Since P_{01} was not given, we cannot check their results. Equation (22) does give, however, the ratio of reflection to transmission locking ranges for a reciprocal two-port oscillator. More comments on their work appear in appendix C.

The final point we address is the variation of power at the two output ports over the locking range. During lock, the injecting signal causes the voltage V_0 to change to $V_0 + \Delta V$. The corresponding change in the device conductance is (see eq. (1))

$$\Delta g = - \frac{G_M}{V_M} \Delta V \tag{23}$$

From reference 11 we know $\Delta V > 0$ for a stable lock. Thus we have from equation (6)

$$\left\{ \left(m^2 Y_0 + n^2 Y_0 - g \right) + \frac{G_M}{V_M} \Delta V \right\} (V_0 + \Delta V) = 2m I_0 \cos \varphi \tag{24}$$

which yields

$$\Delta V = \frac{-G_M V_0 + \sqrt{(G_M V)^2 + 8 G_M V_M m I_0 \cos \varphi}}{2 G_M}$$

we now find P_{out_1} and P_{out_2} during lock by using phasor analysis.

$$P_{out_2} = |\tilde{a}|^2 = n^2 Y_0 |\tilde{V}|^2$$

but $|\tilde{V}|^2 = V^2$

so

$$P_{out_2} = n^2 Y_0 (V_0 + \Delta V)^2 = n^2 Y_0 V_0^2 \left(1 + \frac{\Delta V}{V_0} \right)^2 = P_{02} \left(1 + \frac{\Delta V}{V_0} \right)^2 \tag{25}$$

where $P_{02} = n^2 Y_0 V_0^2$ is the free-running power. For P_{out_1} we find

$$P_{out_1} = |\tilde{a}_2|^2 = \left| \tilde{b} - m\sqrt{Y_0} (\tilde{V} + \Delta \tilde{V}) \right|^2$$

$$= \frac{\left\{ [-I_0 \cos \varphi + m Y_0 (V_0 + \Delta V)]^2 + (I_0 \sin \varphi)^2 \right\}}{Y_0}$$

6

$$= \frac{I_0^2}{Y_0} + m^2 Y_0 V_0^2 \left(1 + \frac{\Delta V}{V_0}\right)^2 - 2m I_0 V_0 \left(1 + \frac{\Delta V}{V_0}\right) \cos \varphi$$

$$= P_{inj} + P_{01} \left(1 + \frac{\Delta V}{V_0}\right)^2 - 2m I_0 V_0 \left(1 + \frac{\Delta V}{V_0}\right) \cos \varphi$$

where

$$P_{inj} = I_0^2 \Big/ Y_0$$

$$P_{01} = n^2 Y_0 V_0^2$$

which we rewrite as

$$P_{out_1} = P_{01} \left(1 + \frac{\Delta V}{V_0}\right)^2 - 2 \sqrt{P_{01} P_{inj}} \left(1 + \frac{\Delta V}{V_0}\right) \cos \varphi + P_{inj} \qquad (26)$$

Kurokawa has shown a stable locking situation requires

$$\frac{\Delta A}{A_0} = 2 \sqrt{\frac{P_{inj}}{P_0}} \frac{\cos \varphi}{S} \qquad (27)$$

where A_0, ΔA are the stable free-running current and current increase after lock. This applies for a single load as shown in figure A-1, where the device has been modeled as a negative impedance $-\bar{Z}(A)$. We assume this condition holds for our case. The modifications for equation (27) are: $\Delta V/V_0$ replaces $\Delta A/A_0$, and P_0 is replaced by the total power absorbed in both loads. Thus we assume

$$\frac{\Delta V}{V_0} = 2 \sqrt{\frac{P_{inj}}{(P_{01} + P_{02})}} \frac{\cos \varphi}{S} \qquad (28)$$

7

Manipulating equation (26)

$$P_{out_1} = P_{01} \left[1 + 2\,\frac{\Delta V}{V_o} + \left(\frac{\Delta V}{V_o}\right)^2 \right] - 2\sqrt{P_{01} P_{inj}}\left(1 + \frac{\Delta V}{V_o}\right)\cos\varphi + P_{inj}$$

$$\doteq P_{01} + 2P_{01}\,\frac{\Delta V}{V_o} - 2P_{01}\sqrt{\frac{P_{inj}}{P_{01}}}\cos\varphi$$

$$= P_{01} + 2P_{01}\left[2\sqrt{\frac{P_{inj}}{(P_{01}+P_{02})}}\,\frac{\cos\varphi}{S}\right] - 2P_{01}\sqrt{\frac{P_{inj}}{P_{01}}}\cos\varphi$$

$$= P_{01} + 2P_{01}\sqrt{\frac{P_{inj}}{P_{01}}}\left[\frac{2}{S\sqrt{1 + \frac{P_{02}}{P_{01}}}} - 1\right]\cos\varphi \qquad (29)$$

which reduces to Kurokawa's result (refs. 9 and 11) when the second port is eliminated ($P_{02} \to 0$). Working on P_{out_2} gives

$$P_{out_2} = P_{02}\left(1 + 2\,\frac{\Delta V}{V_o} + \left(\frac{\Delta V}{V_o}\right)^2\right)$$

$$\doteq P_{02} + 2P_{02}\left[2\sqrt{\frac{P_{inj}}{(P_{01}+P_{02})}}\,\frac{\cos\varphi}{S}\right] \qquad (30)$$

Finally

$$\left(P_{out_2} - P_{02}\right) \overset{\Delta}{=} \Delta P_2 = 2P_{02}\sqrt{\frac{P_{inj}}{P_{01}}}\left[\frac{2}{S\sqrt{1 + \frac{P_{02}}{P_{01}}}}\right]\cos\varphi \qquad (31)$$

$$\left(P_{out_1} - P_{01}\right) \overset{\Delta}{=} \Delta P_1 = 2P_{01}\sqrt{\frac{P_{inj}}{P_{01}}}\left[\frac{2}{S\sqrt{1 + \frac{P_{02}}{P_{01}}}} - 1\right]\cos\varphi \qquad (32)$$

These variations in output power ΔP_1, ΔP_2 are known to be elliptical to first order (ref. 11). For our case these "locking ellipses" may be both concave up or concave down if $S\sqrt{1 + P_{02}/P_{01}} < 2$. However if $S\sqrt{1 + P_{02}/P_{01}} > 2$, the ellipses will be flipped with respect to one another. The quantity S is the original saturation parameter introduced by Edson. In Kurokawa's notation

$$-S = \frac{A_0}{R_0} \frac{\partial \bar{R}}{\partial A} \Bigg|_{A_0} \qquad (33)$$

which for our case becomes

$$S = - \frac{V_0}{(m^2 + n^2)Y_0} \frac{\partial \bar{g}}{\partial V} \Bigg|_{V_0} \qquad (34)$$

We may incorporate device reactance variation with voltage $j\bar{B}(V)$ in the following manner. If for example in equation (18) we define

$$\frac{1}{Q_{ex_2}} = \omega_0 L n^2 Y_0 \qquad (35)$$

then the equation appears as the standard form used in injection locking work.

$$BW_{RL}^{(2)} = \frac{\omega_0}{Q_{ex_2}} \sqrt{\frac{P_{inj_2}}{P_{02}}} \qquad (36)$$

Kurokawa has shown (ref. 9) that reactance effects may be incorporated by multiplying Q_{ex_2} by the factor $\left[1 + (r/S)^2\right]^{-1/2}$ where r is the reactance saturation factor. In Kurokawa's notation this is

$$r = \frac{A_0}{R_0} \frac{\partial \bar{X}}{\partial A} \Bigg|_{A_0} \qquad (37)$$

which for our case becomes

$$r = \frac{V_0}{(m^2 + n^2)Y_0} \frac{\partial \bar{B}}{\partial V} \Bigg|_{V_0} \qquad (38)$$

EXPERIMENTAL SET-UP AND OSCILLATOR PERFORMANCE

The objective of the experiments was to measure and compare the locking bandwidths obtainable when the oscillator was reflection locked versus transmission locked. See figures 4 and 5 for schematics of the measuring setup, and the basic idea of the locking processes. Figure 5(a) depicts a normal locking arrangement, herein referred to as reflection locking (RL). In part (b) the

9

oscillator has two separate output ports and may be locked from either one. The oscillating diode was a flat-profile Si single drift IMPATT.

The procedure here is to first establish the relative output levels to be nearly equal or up to about a 10 dB difference. We then injection lock from channels A and B in turn. If the injection signal originates in channel A, then the reflection locking gain (RL) is $P_{out_1} - P_{inj}$ (both in dBm) and the transmission locking gain (TL) is $P_{out_2} - P_{inj}$.

The IMPATT diode was used in the Kurokawa-type configuration. The outputs were formed by variable irises on the cavity sidewalls (see fig. 6). A copper tuning screw on the wall opposite the coaxial line enabled small adjustments in power and frequency to be made. The cavity dimensions were those for WR-42 waveguide. Three separate experiments were performed. The first had unequal power distribution; P_{out-A} = +7.4 dBm and P_{out-B} = +2.0 dBm. The irises were 0.147 and 0.120 in. respectively. The results are presented in figures 7 to 10. We observe that TL gives a larger locking range than RL when locked from channel B. The situation is reversed when locked from channel A (see fig. 7). Next, each iris was replaced in turn with a short; the characteristics are given in figure 8. Here the effective Q_{ex} stays practically constant since the curves are linear, even though the locking is not in the small signal regime. Figure 9 combines the results of the two previous ones. Note that the locking bandwidth for transmission locking is larger than that for reflection only for channel B. This is similar to the result found in reference 7. The situation is reversed for channel A, which is a result not previously published. The power ratio between the ports when free running was 5.4 dB.

The second experiment used a ratio of 13.2 dB between output power levels when free running. The results are qualitatively similar to those of the previous case as seen from figure 10. Also shown in this figure are curves when locking from channel B was not possible. A slight adjustment of the tuning screw reduced the output of channel B such that sufficient locking power was not available from the sweeper. The results of the final experiment are displayed in figure 11. Here both irises are nearly equal ~0.146 in., and the outputs differ by only 0.5 dB when free running. The reflection and transmission locking bandwidths are nearly equal and practically the same for injected power from either channel.

A typical pair of locking ellipses is shown in figure 12. The photos show the flipping of the ellipses as the injection signal is moved from one port to the other. The fact that the ellipses are of opposite curvature in a given photo means

$$S \sqrt{1 + \frac{P_{02}}{P_{01}}} > 2$$

for our tuning condition.

10

RESULTS AND DISCUSSION

The transmission locking bandwidth is the same, for the same locking gain, when locked from either channel. This experimental result agrees with equation (21) which helps justify the model used. This result holds regardless of the relative output power levels when the device is free running. The TL bandwidth is larger than the one for RL when the lower free running output channel is the side at which the injected signal is applied. Just the opposite case occurs when injected from the other port.

The locking ellipses (ref. 11) were monitored and the results are interesting. For a given tuning condition suppose the ellipse on channel A was concave up, then that on channel B would be concave down. If now the injected signal is switched to the other channel, the ellipses switch, i.e., concave up goes to concave down and vice-versa.

Unlike the FET oscillators discussed in reference 3, the oscillator is reciprocal between its output ports, and there is no great advantage to transmission locking in this case.

APPENDIX A - REVIEW OF INJECTION LOCKED OSCILLATORS

In most cases, oscillators are injection locked by introducing the locking signal via a circulator as shown in figure A-1. The circulator plays a key role in that it separates the output power from the injecting source, as well as providing matched loads for both the injection source and the locked, or free-running, oscillator. A simple lumped equivalent circuit is also shown in the figure, and our initial task is to show that the lower one is indeed correct. We designate all traveling waves as incident if they enter the circulator. Thus V_1^+ is the wave from the locking source, whereas V_3^- is treated as a reflected wave on the termination arm of the circulator. All lines are of characteristic impedance R_0 and are matched to the circulator.

A simple argument can be given to justify the lumped equivalent. Since the locking source sees a matched load

$$V_1^+ = \frac{e}{2}$$

Then if plane $a - a'$ is open circuited the voltage developed is $V_1^+ + \Gamma V_1^+$ since the ideal circulator simply transmits the wave from arm 1 to arm 2. But $\Gamma = +1$ for an open, so the open circuit voltage V_{oc} is

$$V_{oc} = 2V_1^+ = e \tag{A1}$$

If we apply a generator with internal impedance at plane $a - a'$ it sees a match so the input impedance is R_0. Thus the Thevenin equivalent is correct.

From transmission line theory and with the reference direction for I and I' we have

$$V_2^+ = \frac{V - IR_0}{2R_0} \tag{A2}$$

$$V_3^- = \frac{V' - I'R_0}{2R_0} \tag{A3}$$

But the circulator causes $V_3^- = V_2^+$, so

$$V - IR_0 = V' - I'R_0$$

We observe $V' = -I'R_0$ so the above is

$$V - IR_0 = -2I'R_0 \tag{A4}$$

We may apply the voltage law about the contour to find

$$V_1^+ = V - V' = V + I'R_0 \tag{A5}$$

12

Using equations (A1) and (A4) reduces the above to

$$V = e - IR_0 \qquad (A6)$$

which again verifies the simple lumped equivalent. Equation (A5) may be expressed in another form by noticing $I_1^+ = e/2R_0$ and using equations (A1) and (A6). These substitutions give

$$I_1^+ + I' = I \qquad (A7)$$

which is a node-like equation. This relationship between currents is valid only for the designated reference directions used in the figure. By inspection the power leaving the generator is the available value (since the generator is matched),

$$P_{AVAIL} = \frac{|e|^2}{8R_0} \qquad (A8)$$

It is useful to model the active device as a negative conductance in parallel with a resonant circuit as depicted in figure A-2. The resonator and active element are coupled to the circulator via the ideal transformer. The turns ratio m depends on both physical dimensions of the microwave cavity as well as the frequency of the locking signal. We, however, will assume it is a constant to first order. For any particular arm of the circulator we have

$$V_1 = V_1^+ + V_1^- \qquad (A9)$$

$$I_1 = \left(V_1^+ - V_1^-\right)Y_0 \qquad Y_0 = \frac{1}{R_0} \qquad (A10)$$

from basic transmission line theory. We define

$$a_1 = V_1^+ \sqrt{Y_0} \qquad (A11)$$

$$b_1 = V_1^- \sqrt{Y_0} \qquad (A12)$$

then

$$V_1 = \frac{a_1 + b_1}{\sqrt{Y_0}} \qquad (A13)$$

$$I_1 = (a_1 - b_1)\sqrt{Y_0} \qquad (A14)$$

Now the transformer gives

$$-\frac{i_D}{m} = i_2 \qquad (A15)$$

13

and

$$I_2 = (a - b)\sqrt{Y_o} \tag{A16}$$

where I_2 is the phasor representation for i_2. Using the node property (eq. (A7)) we have

$$I_L + I' = -I_2 \tag{A17}$$

By inspection we find

$$I' = (0 - b_3)\sqrt{Y_o}$$

but $b_3 = a_2$. We also notice

$$V_2 \overset{\Delta}{=} mV = \frac{a_2 + b_2}{\sqrt{Y_o}}$$

and

$$b_2 = V_2^-\sqrt{Y_o} = V_1^+\sqrt{Y_o} = \frac{I_L}{Y_o}\sqrt{Y_o} = \frac{I_L}{\sqrt{Y_o}}$$

Using these in equation (A17) yields the desired relationship between I_2 and I_L,

$$2I_L = -I_2 + mVY_o \tag{A18}$$

With the above relations we can now relate i_L and i_D which will yield a useful equivalent circuit. From equations (A18) and (A15)

$$2i_L = +\frac{i_D}{m} + mVY_o$$

or

$$2mi_L = +i_D + m^2VY_o \tag{A19}$$

which is the node equation for the equivalent circuit in figure A-2.

The analysis of the injection locking process proceeds as follows. Define

$$\omega_o = \frac{1}{\sqrt{LC}}$$

$$i_L = I_o \cos \omega t \tag{A20}$$

$$V = V_o \cos (\omega t + \varphi) \tag{A21}$$

14

where the locking current is the reference phasor. We also know

$$i_D = \frac{1}{L} \int V dt + C \frac{dV}{dt} - gV \tag{A22}$$

which when combined with equation (A19) gives

$$\left(m^2 Y_0 - g\right)V + C \frac{dV}{dt} + \frac{1}{L} \int V dt = 2mi_L \tag{A23}$$

which is the fundamental equation relating the device voltage to locking current. Notice V and i_L are defined at different points in the actual circuit, but equation (A23) is the circuit equation for the lumped equivalent circuit. Using the slowly varying assumption for $V_0(t)$ and $\varphi(t)$ we find (ref. 9)

$$\frac{dV}{dt} \simeq -V_0 \left(\omega + \frac{d\varphi}{dt}\right) \sin(\omega t + \varphi) + \frac{dV_0}{dt} \cos(\omega t + \varphi) \tag{A24}$$

$$\int V dt \simeq \left(\frac{V_0}{\omega} - \frac{V_0}{\omega^2}\frac{d\varphi}{dt}\right) \sin(\omega t + \varphi) + \frac{1}{\omega^2}\frac{dV_0}{dt} \cos(\omega t + \varphi) \tag{A25}$$

Multiplying these by $\sin \omega t$ and $\cos \omega t$ in turn and integrating over the rf period $T = 2\pi/\omega$ we find

$$\left(m^2 Y_0 - g\right)V_0 + C \frac{dV_0}{dt} + \frac{1}{\omega^2 L}\frac{dV_0}{dt} = 2mI_0 \cos \varphi \tag{A26}$$

$$-CV_0 \left(\omega + \frac{d\varphi}{dt}\right) + \frac{1}{\omega^2 L}\left(\omega V_0 - V_0 \frac{d\varphi}{dt}\right) = 2mI_0 \sin \varphi \tag{A27}$$

where $V_0 = V_0(t)$ is slowly varying and assumed nearly constant over the interval $(0,T)$. For steady-state conditions

$$-CV_0 \omega + \frac{V_0}{\omega L} = 2mI_0 \cos \varphi$$

$$-\omega C + \frac{1}{\omega L} = \frac{2mI_0}{V_0} \sin \varphi$$

and after using $(\omega_0 + \omega) \simeq 2\omega$, we find

$$(\omega_0 - \omega) \doteq \frac{\omega_0 I_0}{Q_{ext} m Y_0 V_0} \sin \varphi \tag{A28}$$

$$Q_{ext} \overset{\Delta}{=} \frac{1}{\omega_0 L m^2 Y_0} \tag{A29}$$

15

It is customary to express the "injection vector" I_0/V_0 in terms of free-running outpower P_{out} and the injected signal power P_{inj}. The output power is

$$P_{out} = |a_2|^2 \doteq (mV_0)^2 Y_0$$

where

$$mV_0 = \frac{a_2 + b_2}{\sqrt{Y_0}} \qquad (A30)$$

and we have neglected b_2 in equation (A30); this means the injected level is much less than P_{out}. The injected level is

$$P_{inj} = \frac{I_0^2}{Y_0}$$

so

$$\frac{P_{inj}}{P_{out}} = \frac{I_0^2}{m^2 V_0^2 Y_0^2}$$

or

$$\frac{I_0}{V_0} = mY_0 \sqrt{\frac{P_{inj}}{P_{out}}} \qquad (A31)$$

Then we finally obtain

$$\omega_0 - \omega \simeq \frac{\omega_0}{Q_{ext}} \sqrt{\frac{P_{inj}}{P_{out}}} \sin \varphi \qquad (A32)$$

which is a basic relation in injection locking, and is sometimes referred to as Adler's locking equation. At one extreme of the locking range when $\sin \varphi = 1$ we have

$$\omega_0 - \omega \overset{\Delta}{=} \Delta\omega = \frac{\omega_0}{Q_{ext}} \sqrt{\frac{P_{inj}}{P_{out}}} \qquad (A33)$$

and the total locking range (LR) is thus $2\Delta\omega$. The above situation may be simply understood by referring to figure A-3. The equivalent circuit is at the IMPATT terminals. The microwave circuit and injection signal are modeled in the Norton form. The upper admittance plot depicts the steady-state oscillation condition with the injection source removed. The load admittance divisions correspond to equal increments of frequency ω. The "device line" $Y(V)$ represents the effective IMPATT admittance as a function of its terminal voltage V. The intersection of the loci at (ω_0, V_0) determines the steady free-running conditions. The lower figure shows the condition during lock.

The magnitude and angle of the "injection vector" are shown. The tips of this vector determine both the instantaneous amplitude and frequency during a locked condition. The various orientations the vector may assume under stable small injection locking conditions are explained in (ref. 11).

APPENDIX B - REVIEW OF TAJIMA AND MISHIMA

Tajima and Mishima (refs. 3 to 6) embedded an FET oscillator between 50 Ω input and output loads. A microstrip matching network in the drain coupled most of the oscillator power into the load (P_{02}). The gate was connected directly to 50 Ω wherein P_{01} was dissipated. The direct termination at the gate stabilized the oscillation as well as eliminated hysteresis during tuning. Generally P_{01} was 1/7 to 1/9 of P_{02}. The schematic is shown in figure B-1(a). The matching was performed with a quarter wave 90 Ω line in series with a short section of 50 Ω line. The LC network from drain to gate provided the necessary feedback for oscillation. Part (b) gives the simplified equivalent circuit. The experimental schematic is shown in figure B-2, note the FET oscillator is between planes 1 and 2 which are also given in figure B-1. The precision variable attenuators serve to provide both the 50 Ω terminations as well as setting the injection levels. When the injection signal is applied to the drain port, attenuator 2 is reduced from its maximum setting to permit a small injection signal to pass. Attenuator 1 is set to its maximum to provide the largest return loss on the gate port. Just the reverse conditions apply when locking from the gate. The attenuators serve the same purpose as does a circulator, namely to separate oscillator power from the injection source. Care, however, is necessary with the attenuator method. One cannot arbitrarily open an attenuator, for then the injection source is looking into the oscillator directly and will see a negative real part in the impedance. Exactly what would occur in such a condition is impossible to predict, since the FET oscillator may or may not continue to oscillate. Also the pulling of the injection source is not easily predicted. Therefore in any practical situation, the oscillator and injecting source are isolated by either attenuators, isolators, or circulators.

The simplest basic oscillator equivalent circuit with injection source is depicted in figure B-3. The active device is modeled as $Y_a(A)$, where A is the amplitude of V_2. For this case V_2 will represent the voltage at the drain plane. Their primary result is depicted in figure B-4. In part (a) the injection source I is applied at the drain and the simplified network is shown below. In part (b) the same injection source is now applied to the gate. Some analysis shows that this case can be reduced to the simplified circuit shown at the bottom. Notice the situation is similar to that in part (a), with the change being that I is modified to Ieq, where $Ieq = I[-Y_{21}/(Y_{11} + Y_1)]$. It will be shown that the locking range (LR) is directly proportional to the magnitude of the equivalent injection current source when that source is applied at the drain. Thus TL should provide a larger LR than RL by the factor $|-Y_{21}/(Y_{11} + Y_1)|$. In their experiments they were able to achieve an increase of 2.5 of TL over RL.

We start the detailed analysis with reference to figure B-3. A node equation yields

$$[Y_a(A) + Y_L(\omega)]V_2 = I \qquad (B1)$$

where

$$V_2(t) = A \cos(\omega t + \varphi)$$

$$i(t) = I \cos(\omega t) = Re\left\{Ie^{j\omega t}\right\}$$

18

The free-running condition ($I = 0$, $V_2 \neq 0$) is

$$Y_a(A) + Y_L(\omega) = 0 \tag{B2}$$

Our analysis then boils down to studying the equivalent circuit in figure B-3. When RL is used, $I = I$; and when TL occurs, I is replaced by I_{eq}. In part (a) of figure B-4 we find

$$\frac{I_2}{V_2} = Y_a(A) = Y_{22} - \frac{Y_{12}Y_{21}}{Y_{11} + Y_1} \tag{B3}$$

In part (b) of the figure (upper network) we find

$$\frac{I_2}{V_2} = Y_{22} - \frac{Y_{12}Y_{21}}{Y_{11} + Y_1} + \frac{Y_{21}}{Y_{11} + Y_1}\left(\frac{I}{V_2}\right) \tag{B4}$$

$$= Y_a(A) + \frac{Y_{21}}{Y_{11} + Y_1}\left(\frac{I}{V_2}\right)$$

but $I_2/V_2 = -Y_2$, so

$$-Y_2 = Y_a(A) + \frac{Y_{21}}{Y_{11} + Y_1}\left(\frac{I}{V_2}\right)$$

rearrange

$$[Y_a(A) + Y_2(\omega)]V_2 = -\frac{Y_{21}}{Y_{11} + Y_1} I \tag{B5}$$

which is the justification for the equivalent circuit in part (b). In summary, for identical current sources applied at output and input ports respectively, the "equivalent" injection source to be used in figure B-3 is modified in the latter case, (TLO), by the factor $[-Y_{21}/(Y_{11} + Y_1)]$. Writing equation (B2) as

$$[Y_a(A) + Y_2(\omega)] = \frac{I}{V_2}$$

where the right side is interpreted as the admittance vector due to the injection source I. From Kurokawa (refs. 9 to 11) the magnitude of this "injection vector" is given by;

$$\left|\frac{I}{V_2}\right| \doteq \Delta\omega \left|\frac{\partial Y_2}{\partial \omega}\right| \sin \xi \tag{B6}$$

see figure B-5(a), where purely geometrical arguments have been used. The locking range LR is $2\Delta\omega$, and we write

$$\frac{LR}{\omega_0} = 2 \frac{\Delta\omega}{\omega_0} = \frac{2}{\omega_0 \left|\frac{\partial Y_2}{\partial\omega}\right| \sin\xi} \left|\frac{I}{V_2}\right| \tag{B7}$$

Now equation (B7) is the fundamental relationship relating locking range to the injection source. Normally the magnitude of the injection vector is expressed in terms of output power of the oscillator and the injected power. These are more meaningful quantities at microwave frequencies, and directly measurable. The output power (that absorbed in $Y_2(\omega)$) is

$$P_{02} = \frac{1}{2} G_L |V_2|^2 \tag{B8}$$

where $G_L = Re\{Y_2(\omega)\}$. It is assumed that equation (B8) is valid with or without the application of the injection source. The small change in V_2 from the free-running case to the locked case is generally ignored in this part of the analysis. With reference to figure B-1 the power injected P_{1_2}, for the RL case is related to the equivalent generator i_2 by

$$P_{1_2} = P_{AVAIL} = \frac{|I_2|^2}{8G_L} \tag{B9}$$

The justification of equation (B9) is considered elsewhere in the report. Using equations (B8) and (B9) and setting $I_2 = I$ yields

$$\left|\frac{I}{V_2}\right| = 2G_L \sqrt{\frac{P_{12}}{P_{02}}} \tag{B10}$$

Here $G_L = Re\{Y_2(\omega)\} = 20$ mS. Therefore the half-locking range is

$$\left.\frac{\Delta\omega}{\omega_0}\right|_{RL} = \frac{2G_L}{\omega_0 \left|\frac{\partial Y_2}{\partial\omega}\right| \sin\xi} \sqrt{\frac{P_{12}}{P_{02}}} \tag{B11}$$

where RL reminds us that reflection locking occurs. If we assume the same power is injected in the TL mode, then we immediately augment the above as

$$\left.\frac{\Delta\omega}{\omega_0}\right|_{TL} = \frac{2G_L}{\omega_0 \left|\frac{\partial Y_2}{\partial\omega}\right| \sin\xi} \sqrt{\frac{P_{12}}{P_{02}}} \left|\frac{Y_{21}}{Y_{11} + Y_1}\right| \tag{B12}$$

We now manipulate the above into the form Tajima and Mishima developed. For the basic two-port without the injection source

$$I_2 = Y_{21}V_1 + Y_{22}V_2 = -Y_2V_2$$

or

20

$$V_2 = -\frac{Y_{21}}{Y_{22} + Y_2} V_1$$

or

$$|V_2|^2 = \left|\frac{Y_{21}}{Y_{22} + Y_2}\right|^2 |V_1|^2 \tag{B13}$$

but

$$P_{01} = \frac{1}{2} Y_1 |V_1|^2 \tag{B14}$$

where P_{01} is the power absorbed at port 1 (gate). Then

$$|V_2|^2 = \left|\frac{Y_{21}}{Y_{22} + Y_2}\right|^2 \left(\frac{2P_{01}}{Y_1}\right)$$

Multiply by $(1/2)G_L$

$$\frac{1}{2} G_L |V_2|^2 = P_{02} = \left(\frac{G_L}{Y_1}\right) \left|\frac{Y_{21}}{Y_{22} + Y_2}\right|^2 P_{01} \tag{B15}$$

The oscillation condition (eq. (B2)) is

$$Y_{22} - \frac{Y_{12}Y_{21}}{Y_{11} + Y_1} + Y_2 = 0$$

or

$$(Y_1 + Y_{11})(Y_2 + Y_{22}) = Y_{12}Y_{21} \tag{B16}$$

so equation (B15) may be written as

$$P_{02} = \left(\frac{G_L}{Y_1}\right) \left|\frac{Y_1 + Y_{11}}{Y_{12}}\right|^2 P_{01} \tag{B17}$$

or

$$|Y_1 + Y_{11}| = |Y_{12}| \sqrt{\frac{Y_1}{G_L}} \sqrt{\frac{P_{02}}{P_{01}}}$$

21

Using this in equation (B12) yields

$$\left.\frac{\Delta\omega}{\omega_0}\right|_{TL} = \frac{2G_L}{\omega_0 \left|\frac{\partial Y_2}{\partial\omega}\right| \sin\xi} \sqrt{\frac{P_{12}}{P_{02}}} \left|\frac{Y_{21}}{Y_{12}}\right| \sqrt{\frac{G_L}{Y_1}} \sqrt{\frac{P_{01}}{P_{02}}}$$

$$= \frac{2G_L}{\omega_0 \left|\frac{\partial Y_2}{\partial\omega}\right| \sin\xi} \frac{G_s}{G_p} \sqrt{\frac{P_{12}}{P_{02}}} \qquad (B18)$$

where

$$G_s \equiv \left|\frac{Y_{21}}{Y_{12}}\right| \qquad (B19)$$

$$G_p \equiv \sqrt{\frac{P_{02}}{P_{01}}} \qquad (B20)$$

and

$$G_L = Y_1 \qquad (B21)$$

The condition $G_L = Y_1$ is a necessary condition imposed by the experiments as well as the assumed equivalent circuits. If we define (ref. 12) (assume $\partial G_L/\partial\omega = 0$ so $\partial Y_2/\partial\omega = \partial B_2/\partial\omega$, $Y_2 \equiv G_L + jB_2$)

$$Q_{ext} = \frac{\omega_0}{2G_L} \left|\frac{\partial Y_2}{\partial\omega}\right|_{\omega_0} \qquad (B22)$$

we finally have

$$\left.\frac{\Delta\omega}{\omega_0}\right|_{TL} = \frac{1}{Q_{ext}} \frac{G_s}{G_p} \sqrt{\frac{P_{12}}{P_{02}}} \frac{1}{\sin\xi} \qquad (B23)$$

which is equation (7) in reference 4. Comparing equations (B11) and (B23) yields

$$\frac{LR_{TL}}{LR_{RL}} = \frac{G_s}{G_p} = \left|\frac{Y_{21}}{Y_{12}}\right| \sqrt{\frac{P_{01}}{P_{02}}} \qquad (B24)$$

which is their basic result.

We may summarize their experimental results as follows. In one experiment at 9.2 GHz, they obtained

$$P_{02} = +10 \text{ dBm}$$

$$\frac{P_{02}}{P_{01}} = \frac{7}{1} \Rightarrow G_p = 2.65$$

$$G_s(\text{meas.}) = \left| \frac{Y_{21}}{Y_{12}} \right| = \left| \frac{S_{21}}{S_{12}} \right| = 3.34$$

$$\frac{LR_{TL}}{LR_{RL}} \overset{\Delta}{=} n_{TR} = 1.26 \text{ (calc.)}$$

$$= 1.21 \text{ (meas.)}$$

$$14 \text{ dB} < \frac{P_{02}}{P_1} < 34 \text{ dB}$$

It is not clear, nor was it specified, how the small-signal G_s was measured. First of all small signal G_s will not be appropriate during oscillation wherein large signal conditions prevail. Apparently they reduced the drain current just enough to quench the oscillation and then measured S_{12} and S_{21}. Note that these include the external LC feedback network. In another experiment at 8.1 GHz they found

$$P_{02} = 18.3 \text{ mW}$$

$$P_{01} = 4.5 \text{ mW} \qquad \left(\frac{P_{02}}{P_{01}} = \frac{4}{1} \right)$$

$$n_{TR} = 1.5 \text{ (meas.)}$$

$$\left. \begin{array}{l} Q_{ex_1} = 10.5 \\ \\ Q_{ex_2} = 15.3 \end{array} \right\} \text{These are discussed later.}$$

$$20 \text{ dB} < \frac{P_{02}}{P_1} < 55 \text{ dB}$$

$$2 \text{ MHz} < LR < 100 \text{ MHz}$$

The last case reported had

$$P_{02} = 30 \text{ mW}$$

$$P_{01} = \frac{30}{9} \text{ mW}$$

$$\eta_{TR} = 1.8 \text{ (meas.)} \quad \text{when} \quad \frac{P_{02}}{P_{i_2}} = \frac{P_{01}}{P_{i_1}}$$

$$Q_{ex_1} = 16$$

$$Q_{ex_2} = 9$$

The FM noise was lower for TL when the condition $P_{02}/P_{i_2} = P_{01}/P_{i_1}$ was imposed. Also they claimed lower FM noise with TL with the same injected level; i.e., $P_{i_1} = P_{i_2}$.

Some of the benefits they mentioned for a two-port oscillator included using it as a self-oscillating mixer when the locking signal was too far away in frequency to obtain synchronization. This property could be useful in a doppler detector. The largest η_{TR} observed was 2.5.

With their basic results now well understood we proceed to criticize some of their misleading statements. Starting with reference 6 one must notice the equivalent circuit presented there is different from that in the other papers. The circuit schematic is given in figure B-6. Comparison with figure B-1(b) reveals V_2 is now that across plane 2 rather than the drain. Thus Y_S and Y_L are assumed pure real (and here both are 20 mS). The admittance $Y_T(\omega,A)$ is that looking into the gate from the plane of the 50 Ω gate load (plane 1). The amplitude of V_1 is now A. The term $Y_u(\omega,B)$ is that looking into the drain port (plane 2) which includes the drain matching network. Here B is the amplitude of V_2. Using the general approach of Kurokawa they develop

$$\left. \frac{\Delta\omega}{\omega_0} \right|_{TL} = \frac{1}{Q_{ext_1}} \sqrt{\frac{P_{i_1}}{P_{02}}} \tag{B25}$$

$$\left. \frac{\Delta\omega}{\omega_0} \right|_{RL} = \frac{1}{Q_{ext_2}} \sqrt{\frac{P_{i_2}}{P_{02}}} \tag{B26}$$

They claim (without proof, although they allude to how the proof was developed in their appendix),

$$\frac{Q_{ext_2}}{Q_{ext_1}} = \frac{G_s}{G_p} \tag{B27}$$

which yields

$$\frac{LR_{TL}}{LR_{RL}} = \sqrt{\frac{P_{i_1}}{P_{i_2}}} \frac{G_s}{G_p} \tag{B28}$$

24

and if $P_{i_1} = P_{i_2}$, which is <u>necessary</u> for their analysis to hold

$$\frac{LR_{TL}}{LR_{RL}} = \frac{G_s}{G_p}$$

which is just equation (B24).

Now exactly how Q_{ext_1} and Q_{ext_2} are to be measured (or calculated for that matter is not specified. For example

$$Q_{ext_1} = \frac{\omega_0}{2} \frac{1}{\sqrt{Y_L Y_S}} \left| \frac{Y_{22} + Y_L}{Y_{21}} \right| \frac{|I|}{|V_1|} \Delta\omega \tag{B29}$$

which is not amenable to measurement. The values for Q_{ex_1} and Q_{ex_2} alluded to earlier are apparently the Q_{ext_1} and Q_{ext_2} presented here. Therefore the results in reference 6 are exactly those in the others. However equation (B28) is misleading since $Pi_1 = Pi_2$ always, if the analysis is to hold.

The next, and most misleading concept they present, is the notion that a circulator or isolator may not be necessary to isolate the injection source from the oscillator. The following quote "a big advantage of this injection-locking technique is that it does not require the use of a circulator to isolate the input and output ports and yet still retains high gain $(P_2/P1)$ within a locking range which is wider than that of reflection-type ILOs." may be found in both reference 3 page 304, first paragraph and reference 4, last paragraph of section III. The last sentence of section V in reference 6 says "But, because there is a minimal power loss at the signal input port, an isolator might be necessary between the injection port and signal source." which seems to imply an isolator is <u>not necessary</u>. However, they recant somewhat on this notion in the last line of section II in reference 6. "It will be necessary for most of the system applications to use an isolator in order to isolate the signal source and oscillator." As we have shown, if the injected power and equivalent current source are related by equation (B9), which is necessary for their analysis as well as experimental setup, then a circulator or isolator <u>must</u> <u>be</u> <u>used</u>.

Throughout all of their papers they treat Y_1 and G_L as generally unequal quantities. However, they are always equal, and their value is 20 mS. Further discussion of this point to help clarify our position is developed by referring to figure B-2. While they may have the same level of injection power reaching the gate or drain port, the actual power leaving the injection source may be different, depending on the relative settings of the attenuators. Experimentally it does not seem possible to reduce the attenuation to zero on the locking side, for then the injection source and the oscillator both are looking into negative impedances. In other words the connection is equivalent to two current sources with different values connected in series; a difficult situation. Exactly what would occur in such a situation depends on the saturation behavior of the FET, which is not really addressed here.

The last criticism concerns the admittance plots in references 3 and 4. The matching circuit shown in figure B-1(a) gives $\bar{Z}_{in}$ at the drain plane of 1.41-j1.41, or $\bar{Y}_{in}$ = 0.355+j.35. If this is assumed to be a conjugate match at this plane, then $\bar{Y}_2^*$ = 0.355 - j.35. This point, $\bar{Y}_2^*$ does appear on the "resonant load line" in figure 4 of reference 4. But there is some confusion here. First of all, the oscillation condition is (eq. B2))

$$Y_2(\omega) = -Y_a(A)$$

Thus $R_e\{Y_a(A)\}$ must be a negative number. Therefore $-\bar{Y}_a(A)$ can be plotted on a normal Smith chart, as can $\bar{Y}_2(\omega)$. It appears they have plotted $-\bar{Y}_a^*(A)$ as well as $\bar{Y}_2^*(\omega)$. They indicate the intersection of $-\bar{Y}_a^*(A)$ and $\bar{Y}_2^*(\omega)$ occurs at 0.29-j.17 which is not the point corresponding to $\bar{Y}_2^*(\omega)$. The point $\bar{Y}_2^*(\omega)$ does, however, lie on the "resonant load line" given in their figure. It is not too far from their intersection point.

In summary, their series of papers are somewhat misleading, even though the basic idea is borne out experimentally. For the same injection level, TL can provide a larger locking range than can RL. This increase may be estimated by equation (B24). A major problem with this expression is the accurate measurement of $|Y_{21}/Y_{12}|$. This must be a large signal measurement which would be difficult if not impossible to perform. Apparently one should assume small signal values will yield adequate results.

APPENDIX C - REVIEW OF RAJPUT AND SARKAR

The short note by Rajput and Sarkar (ref. 7) reported results of injection locking a GUNN device in both RLO and TLO configurations. Figure C-1 gives the measurement schematics. The RLO case was said to use a circulator and shorting plunger as shown. The TLO case was not clearly specified except for the fact that a coupling iris replaced the plunger. The LR versus locking gain curve indicated n_{TR} of as much as 7. They said this was even greater than the largest n_{TR} = 2.5 obtained by Tajima and Mishima. Quoting the last line "It is thus concluded that like the GaAs FETs, an oscillating GUNN diode gives better locking gain and locking range when used in transmission type injection-locked configuration."

We do not agree with their conclusions for the following reasons. First of all, the RL and TL measurements were made with the completely different circuit configurations; i.e., plunger versus iris. In the RL case only one load port existed, while the TL case had two ports that each absorbed some power. With this much change it is not surprising different locking ranges were obtained. The expression for a single port LR is

$$\left.\frac{LR}{\omega_0}\right|_{RL} = 2 \left.\frac{\Delta\omega}{\omega_0}\right|_{RL} = 2 \frac{2G_L}{\omega_0 \left|\frac{\partial Y_2}{\partial \omega}\right| \sin \xi} \sqrt{\frac{P1_2}{P_{02}}} \tag{C1}$$

and different configurations can change both ξ and $|\partial Y_2/\partial \omega|$ such that the product $|\partial Y_2/\partial \omega| \sin \xi$ may change by a factor of 7. We feel the latter changes were in part the cause of their results. The notion that a circulator could be eliminated may have been used in the TLO case. If that were the case then the results are not predictable from an analytic model. It is apparent the authors were not aware that the improvement in LR in the TL case is due basically to the $|Y_{21}/Y_{12}|$ ratio being large in the FET configuration. That this ratio is unity in a GUNN device was not addressed. Thus their confusion concerning TL versus RL is easily recognized.

REFERENCES

1. Lazarus, M.J.; and Davis, R.G.: A Two-Port mm-Wave Oscillator. Microwave J., vol. 28, Mar. 1985, pp. 165-170.

2. Davis, R.G.; and Lazarus, M.J.: Phase Locking of mm-Wave Two-Port Gunn Oscillator by Bias Tuning. Microwave J., vol. 29, June 1986, pp. 103-107.

3. Tajima, Y.: GaAs FET Applications for Injection-Locked Oscillators and Self-Oscillating Mixers. 1978 IEEE MTT-S International Microwave Symposium Digest, J.Y. Wang, ed., IEEE, 1978, pp. 303-305.

4. Tajima, Y.: GaAs FET Applications for Injection-Locked Oscillators and Self-Oscillating Mixers. IEEE Trans. Microwave Theory Tech., vol. 27, no. 7, July 1979, pp. 629-632.

5. Mishima, K.; and Tajima, Y.: FM Noise of Transmission-Type Injection-Locked GaAs FET Oscillators and Amplifiers. 1979 IEEE MTT-S International Microwave Symposium Digest, J.E. Tracy, ed., IEEE, 1979, pp. 194-196.

6. Tajima, Y.; and Mishima, K.: Transmission-Type Injection Locking of GaAs Schottky-Barrier FET Oscillators. IEEE Trans. Microwave Theory Tech., vol. 27, no. 5, May 1979, pp. 386-391.

7. Rajput, S.S.; and Sarkar, S.: A Note on Injection-Locked Gunn Oscillators. Int. J. Electron., vol. 52, no. 3, Mar. 1982, pp. 305-306.

8. Sarkar, S.; and Gupta, O.S.: Dependence of Multiple-Device Oscillator Injection-Locking Range on the Number of Constituent Devices. IEEE Trans. Microwave Theory Tech., vol. 34, no. 7, July 1986, pp. 839-840.

9. Kurokawa, K.: An Introduction to the Theory of Microwave Circuits. Academic Press, 1969.

10. Kurokawa, K.: Microwave Solid State Oscillator Circuits. Microwave Devices: Device Circuit Interactions, M.J. Howes and D.V. Morgan, eds., John Wiley, 1976, pp. 209-265.

11. Kurokawa, K.: Injection-Locking of Microwave Solid-State Oscillators. Proc. IEEE, vol. 61, no. 10, Oct. 1973, pp. 1386-1410.

12. Matthai, G.L.; Young, L.; and Jones, E.M.T.: Microwave Filters, Impedance Matching Networks and Coupling Structures, McCraw-Hill, 1964.

13. Hayasaka, T.; Sakamoto, K.; and Tamura, R.: A Study of Injection-Locking and Negative-Resistance Amplifiers. NEC Res. Develop., no. 40, Jan. 1976, pp. 26-36.

14. Shackle, P.W.: A New Technique for the Characterization of Microwave Avalanche Diodes. IEEE Trans. Microwave Theory Tech., vol. 18, no. 11, Nov. 1970, pp. 995-998.
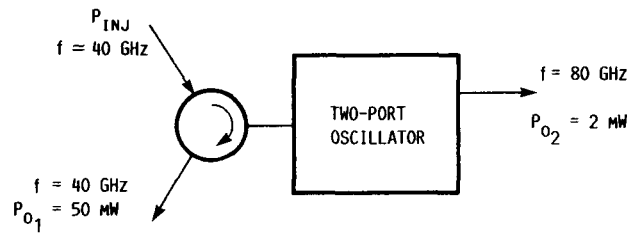
(A) A TWO-PORT GUNN OSCILLATOR WITH OUTPUTS AT 40 GHz AND 80 GHz. SINCE THE MAJOR PORTION OF THE POWER DEVELOPED IS AT 40 GHz, THE 80 GHz COMPONENT IS THE SECOND HARMONIC.
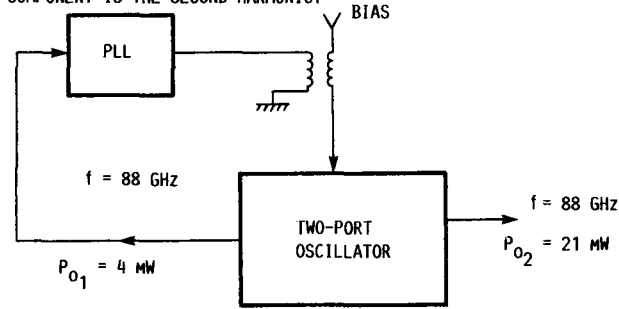
(B) A SELF-STABLIZED CONFIGURATION THAT REDUCES BOTH NOISE AND DRIFT.

FIGURE 1. - EXAMPLES OF USES OF TWO-PORT OSCILLATORS.
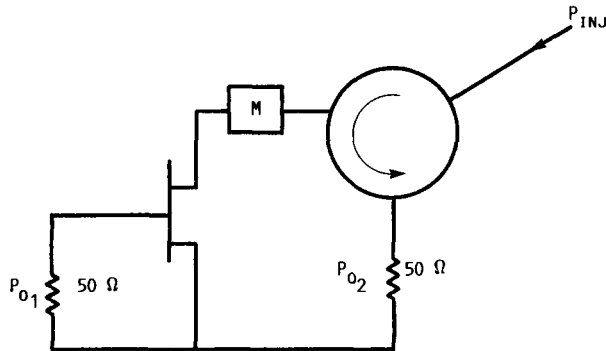
(A) THE CONFIGURATION NAMED REFLECTION LOCKING FOR A TWO-PORT OSCILLATOR, GENERALLY $P_{o_2} \gg P_{o_1}$. WHEN $P_{o_1} \to 0$ THIS REDUCES TO A NORMAL INJECTION LOCKED OSCILLATOR.
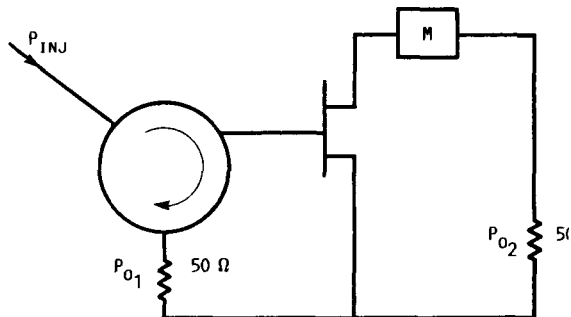
(B) THE TRANSMISSION LOCKING CONFIGURATION IS GIVEN.

FIGURE 2.- THE DEFINITIONS FOR REFLECTION AND TRANSMISSION LOCKING.
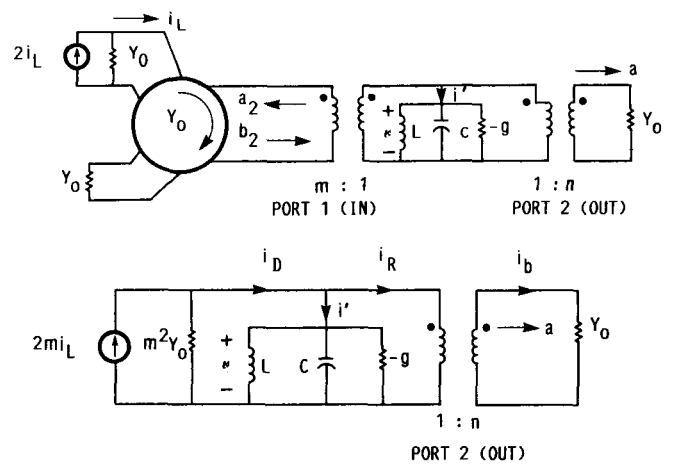
FIGURE 3. - THE SCHEMATIC OF A TWO-PORT INJECTION-LOCKED OSCILLATOR ALONG WITH A LUMPED EQUIVALENT CIRCUIT. TRAVELING WAVES ARE DE-NOTED AS a AND b ON THE VARIOUS TRANSMISSION LINES.

29
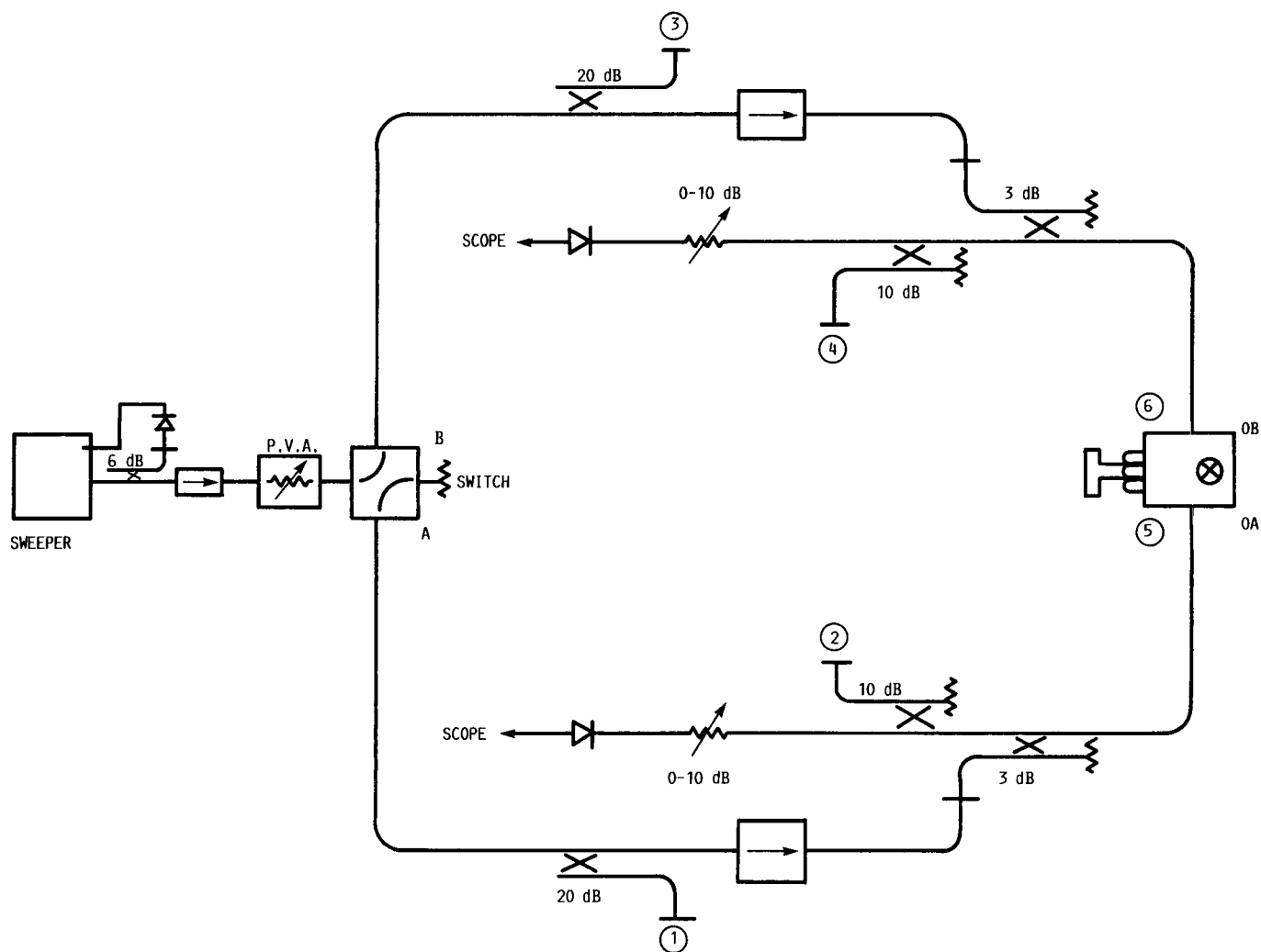
FIGURE 4. - THE TWO-PORT IMPATT OSCILLATOR IS BETWEEN PLANES (5) AND (6). THE ARMS A AND B ARE CONNECTED TO THE MANUAL SWITCH TO PERMIT LOCKING FROM BOTH PORTS SEQUENTIALLY.

(A) NORMAL INJECTION LOCKING (REFLECTION).

(B) TRANSMISSION LOCKING (TL); P_{INJ} NON-ZERO AT ONE PORT ONLY.
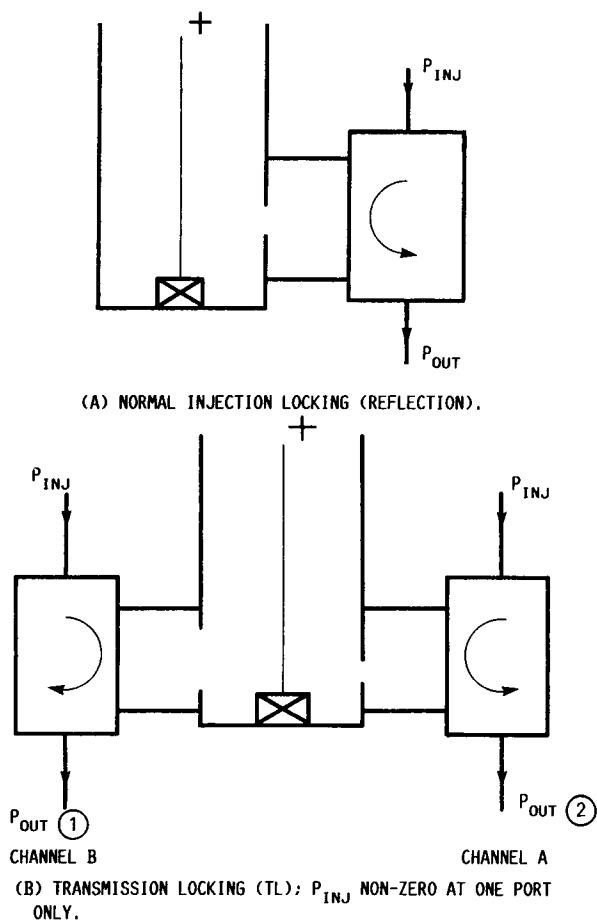
FIGURE 5. – A SIMPLIFIED VIEW OF REFLECTION AND TRANSMISSION LOCKING EXPERIMENTS FOR AN IMPATT DIODE.
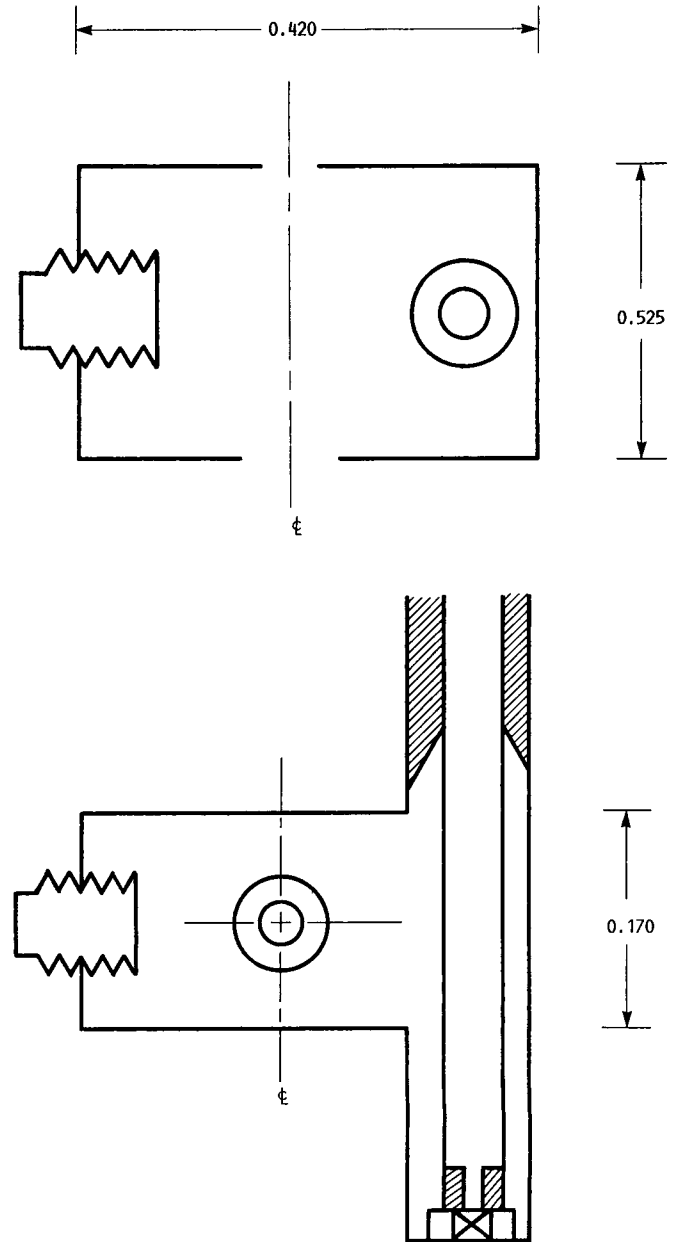
FIGURE 6. – SCHEMATIC OF KUROKAWA-TYPE MICROWAVE CIRCUIT WITH VARIABLE OUTPUT COUPLING IRISES.

f_0 = 18.500405 GHz P_{OUT-A} = + 7.4 dBm
I_D = 130 MA P_{OUT-B} = + 2.0 dBm
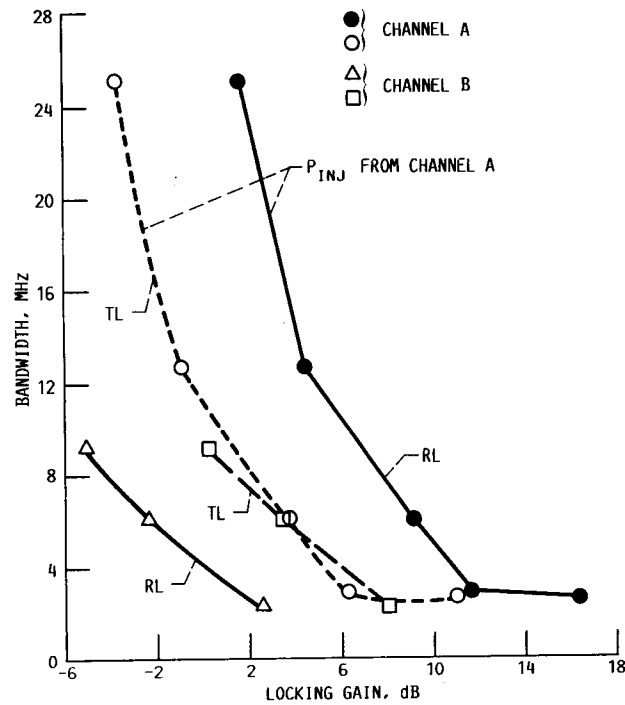
FIGURE 7. - MEASURED LOCKING BANDWIDTH VERSUS LOCKING GAIN
FOR THE TWO-PORT IMPATT DIODE OSCILLATOR.

REFLECTION LOCK WITH ONE IRIS CLOSED I_D = 130 MA
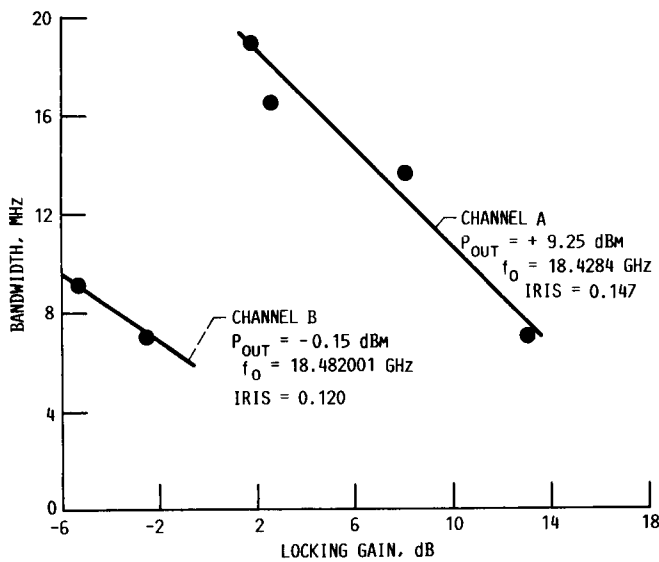
FIGURE 8. - LOCKING BEHAVIOR OF IMPATT OSCILLATOR WHEN ONLY ONE
OUTPUT PORT EXISTS.
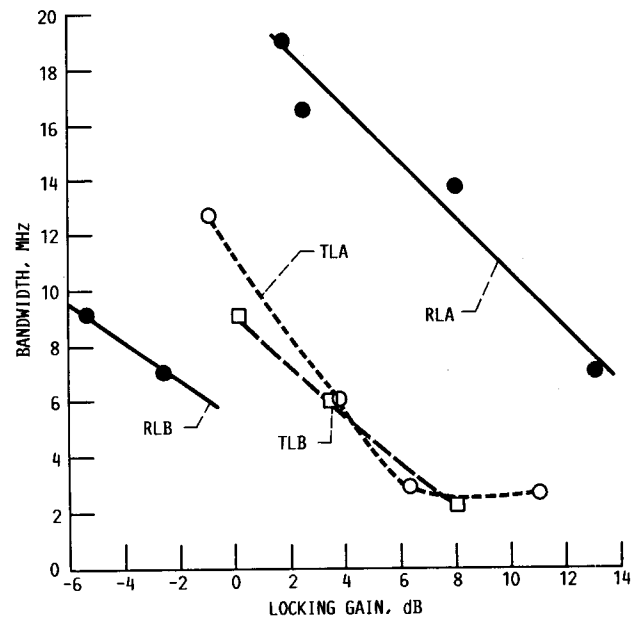
FIGURE 9. - DATA THAT DEMONSTRATES THE EQUIVALENCE OF TRANS-
MISSION LOCKING BANDWIDTHS. ALSO SHOWN ARE THE REFLECTION
LOCKING BANDWIDTHS WHEN THE INJECTION SIGNAL IS ALTERNATELY
APPLIED AT PORTS A AND B.

$f_0 = 18.535$ GHz $P_{OUT-A} = +5.9$ dBm   IRIS = 0.146

$I_D = 130$ mA $P_{OUT-B} = -7.3$ dBm   IRIS = 0.088
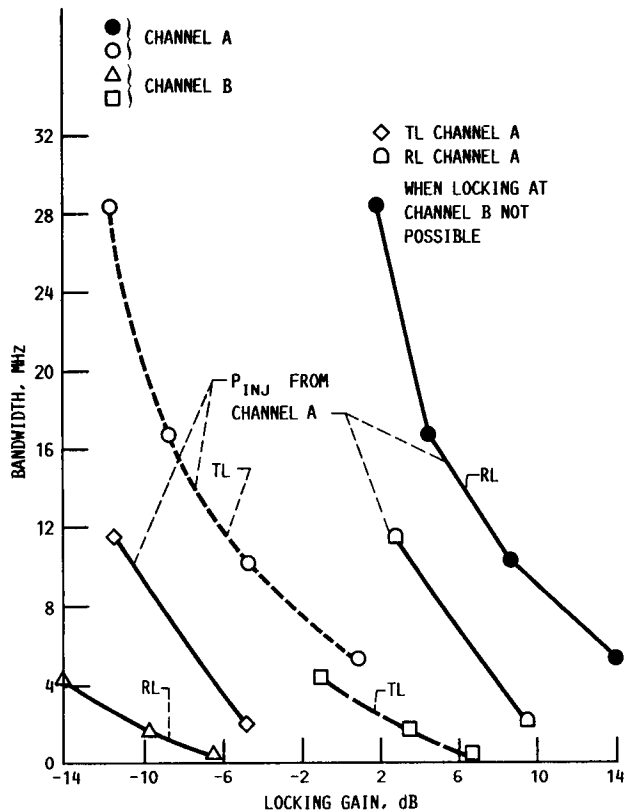
FIGURE 10. - MORE DATA TO DEMONSTRATE THE NEAR EQUIVALENCE
OF TRANSMISSION LOCKING BANDWIDTHS. HERE THE OUTPUT POWER
LEVELS DIFFER BY 13.2 dB WHEN FREE-RUNNING.
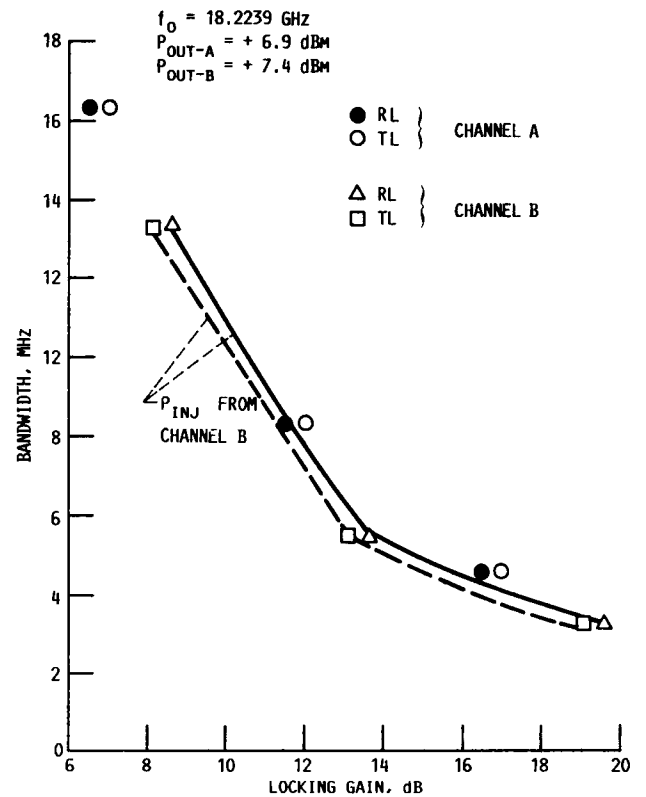
FIGURE 11. - THE CASE WHEN THE FREE-RUNNING OUTPUT LEVELS
ARE REASONABLY CLOSE (0.5 dB DIFFERENCE). ALL OF THE
LOCKING BANDWIDTHS ARE PRACTICALLY THE SAME FOR THE SAME
LOCKING GAIN.
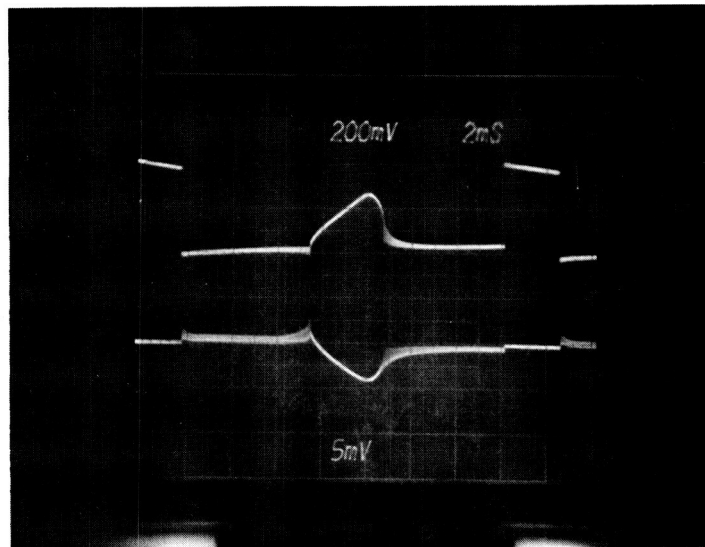
(A) THE LOCKING ELLIPSES ON PORTS A AND B.
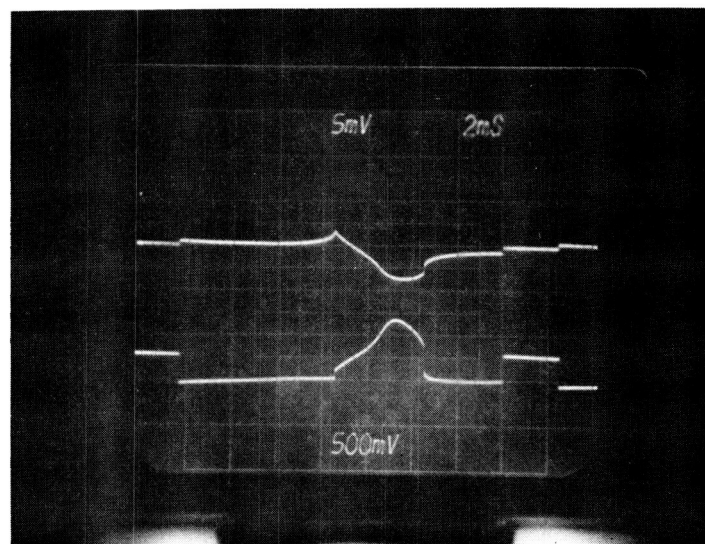
(B) THE ELLIPSES WHEN THE INJECTION SIGNAL IS APPLIED TO THE OPPOSITE
PORT.

FIGURE 12. - A DEMONSTRATION OF THE FLIPPING OF THE LOCKING ELLIPSES AS
THE INJECTION SIGNAL IS APPLIED TO ALTERNATE PORTS. THE DISTORTIONS ARE
DUE TO THE LARGE INJECTED SIGNAL LEVEL TO OBTAIN ADEQUATELY LARGE LOCK-
ING RANGES FOR GOOD MEASUREMENT ACCURACY.
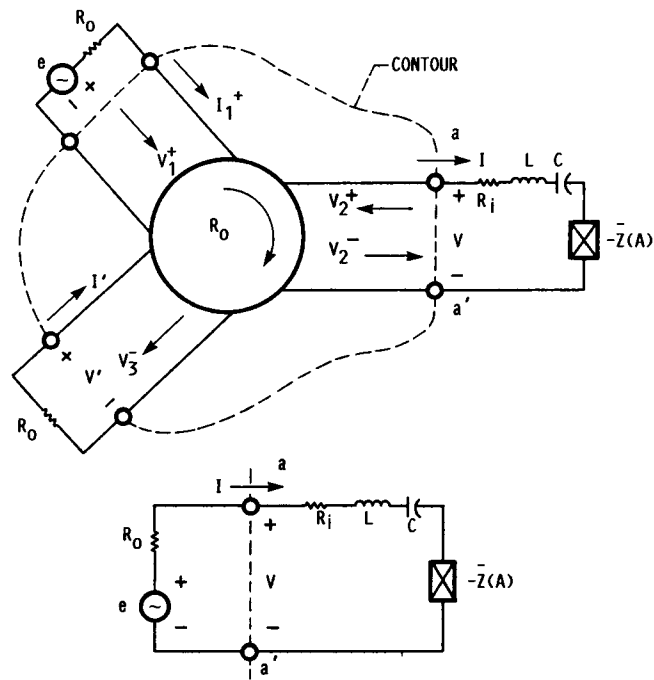
FIGURE A-1. - BASIC SCHEMATIC AND LUMPED EQUIVALENT CIRCUIT FOR INJECTION
LOCKING STUDIES.
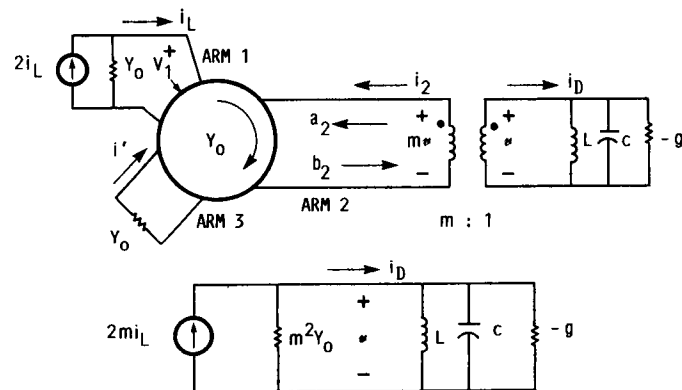
FIGURE A-2. - THE CASE WHEN THE ACTIVE DEVICE IS MODELED AS A NEGATIVE
CONDUCTANCE. THE LUMPED EQUIVALENT APPEARS BELOW THE SCHEMATIC.
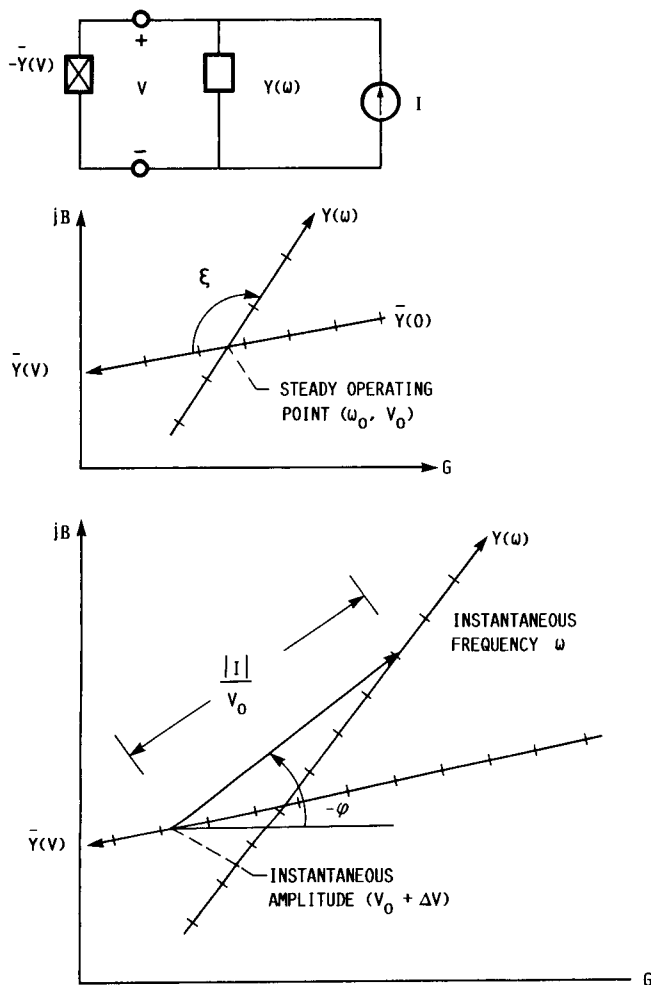
FIGURE A-3. – EQUIVALENT CIRCUIT OF INJECTION-LOCKED OSCILLATOR
ALONG WITH ADMITTANCE PLANE CONSTRUCTIONS USEFUL IN UNDERSTANDING
THE LOCKING PROCESS.
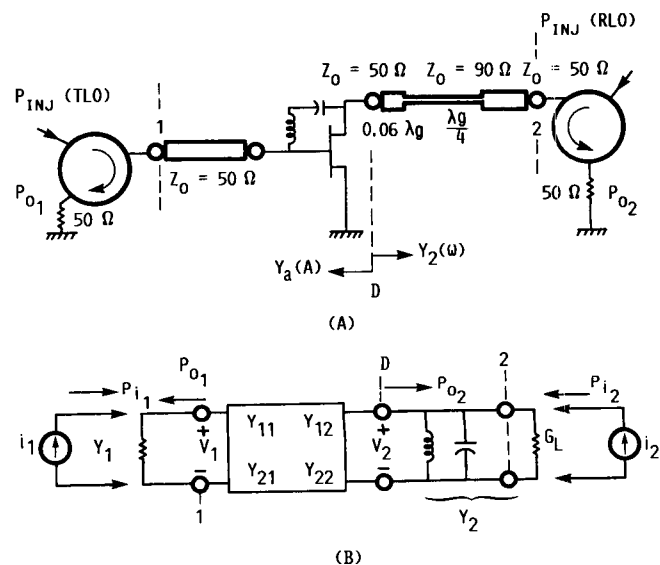
FIGURE B-1. – THE SCHEMATIC AND EQUIVALENT CIRCUIT USED TO STUDY
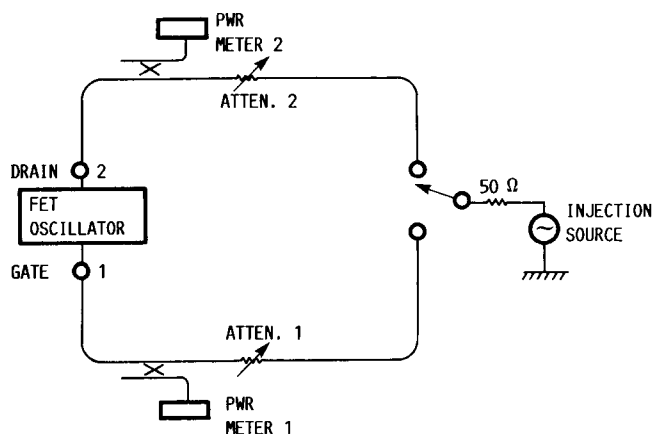LOCKING BEHAVIOR OF A TWO-PORT FET OSCILLATOR.

FIGURE B-2. – THE SIMPLIED SCHEMATIC OF THE EXPERIMENTAL SETUP USED
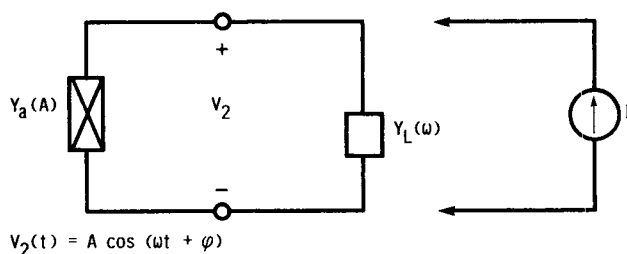TO BOTH REFLECTION AND TRANSMISSION LOCK THE FET OSCILLATOR.

$V_2(t) = A \cos (\omega t + \varphi)$

FIGURE B-3. – BASIC ADMITTANCE MODEL FOR INJECTION LOCKING.
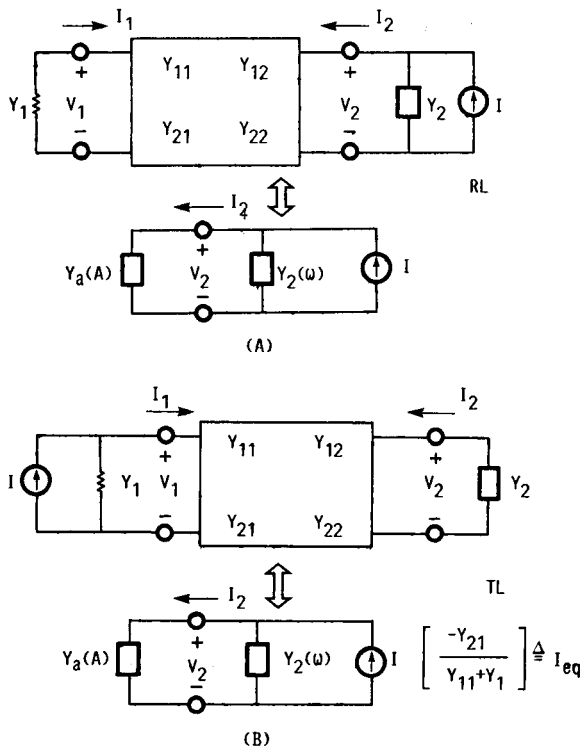
FIGURE B-4. - VARIOUS EQUIVALENT CIRCUITS NEEDED TO ANALYZE
TWO-PORT LOCKING PHENOMENA.

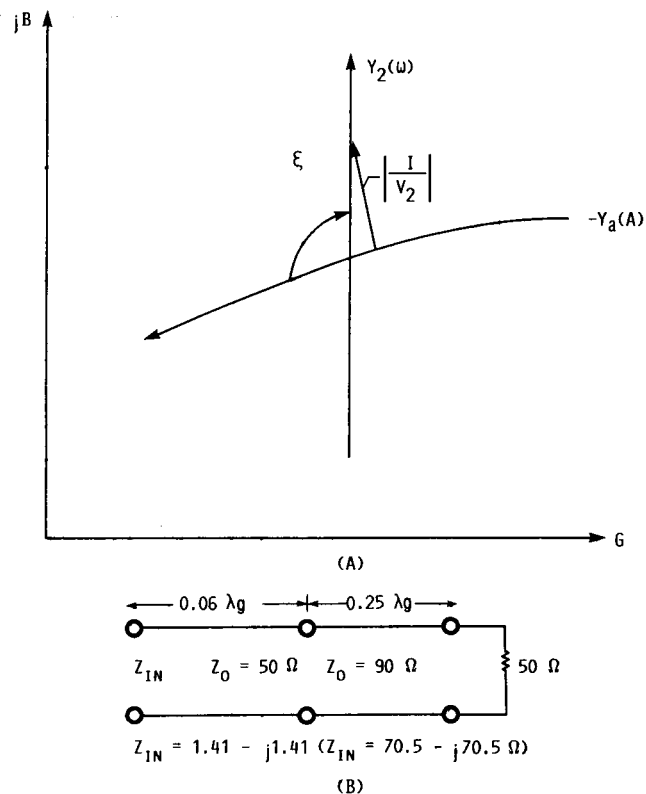

FIGURE B-5. - (A) THE ADMITTANCE PLANE DEPICTION OF $-Y_a(A)$,
$Y_2(\omega)$ AND THE INJECTION VECTOR $|I/V_2|$. (B) THE MATCHING
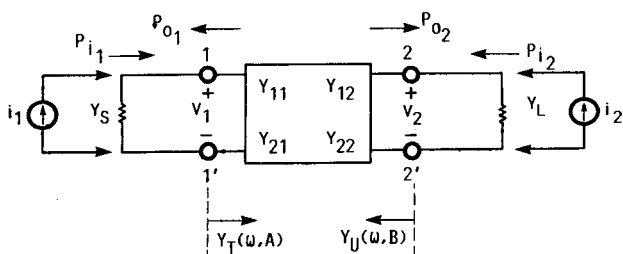NETWORK USED IN THE DRAIN CIRCUIT.

FIGURE B-6. - ALTERNATE Y-PARAMETER REPRESENTATION FOR THE FET
OSCILLATOR. THE REFERENCE PLANES ARE DIFFERENT FROM THOSE
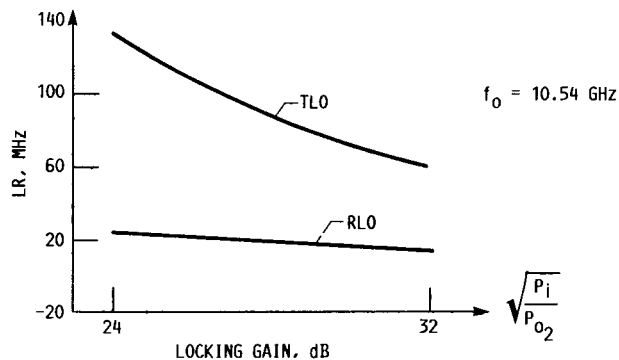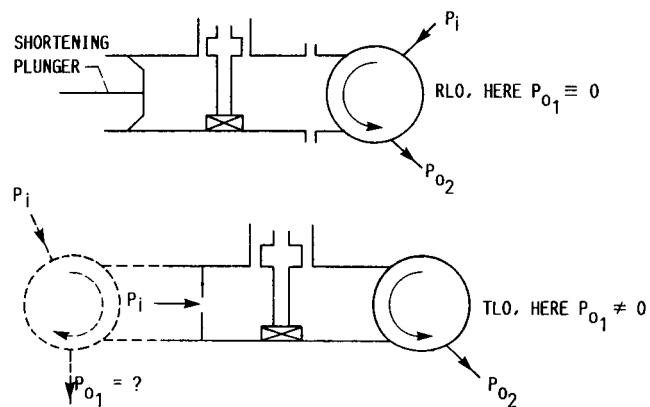USED IN PREVIOUS FIGURES.

FIGURE C-1. - EXPERIMENTAL SETUPS FOR REFLECTION AND TRANSMISSION
LOCKING OF A POST-IN-WAVEGUIDE MOUNTED GUNN DIODE. THE MEASURED
LOCKING BANDWIDTHS ARE SHOWN IN THE LOWER PORTION.

NASA
National Aeronautics and
Space Administration

Report Documentation Page

1. Report No. NASA TM-100119	2. Government Accession No.	3. Recipient's Catalog No.
4. Title and Subtitle An Analytical and Experimental Study of Injection-Locked Two-Port Oscillators		5. Report Date July 1987
		6. Performing Organization Code 679-40-00
7. Author(s) Jon C. Freeman and Alan N. Downey		8. Performing Organization Report No. E-3663
		10. Work Unit No.
9. Performing Organization Name and Address National Aeronautics and Space Administration Lewis Research Center Cleveland, Ohio 44135		11. Contract or Grant No.
		13. Type of Report and Period Covered Technical Memorandum
12. Sponsoring Agency Name and Address National Aeronautics and Space Administration Washington, D.C. 20546		14. Sponsoring Agency Code

15. Supplementary Notes

16. Abstract

A Ku-band IMPATT oscillator with two distinct output power ports was injection-locked alternately at both ports. The transmission locking bandwidth was nearly the same for either port. The lower free running power port had a reflection locking bandwidth that was narrower than its transmission locking one. Just the opposite was found at the other port. A detailed analytical model for two-port injection-locked oscillators is presented, and its results agree quite well with the experiments. A detailed critique of the existing literature on this topic is included to clear up several misconceptions and errors that have appeared in several articles. It is concluded that two-port injection-locked oscillators may prove useful in certain communication systems.

17. Key Words (Suggested by Author(s)) IMPATT oscillators Injection locking	18. Distribution Statement Unclassified - unlimited STAR Category 33

19. Security Classif. (of this report) Unclassified	20. Security Classif. (of this page) Unclassified	21. No of pages 38	22. Price* A03

NASA FORM 1626 OCT 86   *For sale by the National Technical Information Service, Springfield, Virginia 22161